ADVANCED FUNCTIONAL MATERIALS
www.afm-journal.de

www.MaterialsViews.com

Graphene-Oxide-Conjugated Polymer Hybrid Materials for Calmodulin Sensing by Using FRET Strategy

Hongbo Yuan, Junjie Qi, Chengfen Xing, Hailong An, Ruimin Niu, Yong Zhan,* Yibing Fan, Wenmin Yan, Ruihua Li, Bing Wang, and Shu Wang**

The conformation of calmodulin (CaM) changes from closed configuration to open one, converting to a claviform dumbbell-shaped biomolecule upon Ca^{2+}-binding. A hybrid probe of graphene oxide (GO) cationic conjugated polymer for detection of the conformation transition of CaM by using FRET technique is demonstrated. The stronger hydrophobic interaction and weaker electrostatic repulsion leads to more CaM adsorption to the surface of GO upon binding with Ca^{2+} than that of CaM in the absence of Ca^{2+} (apoCaM), resulting in much farther proximity between poly[(9,9-bis(6′-*N*,*N*,*N*-trimethylammonium)hexyl)-fluorenylene phenylene dibromide] (PFP) and green fluorescent protein labeled at the N-terminus of CaM and therefore much weaker FRET efficiency for PFP/Ca^{2+}/CaM in comparison with that of PFP/apoCaM in the presence of GO. Notably, the assembly of CaM with GO is quantitatively and reversibly controlled by Ca^{2+} ions.

1. Introduction

As a cellular Ca^{2+}-binding protein of 148 amino acid residues, calmodulin (CaM) mediates a large number of Ca^{2+}-dependent signal transductions, regulating activities of a variety of proteins including CaM kinases and ion channels.[1] CaM consists of two globular domains at C- and N-terminus and each contains two canonical EF hands as Ca^{2+}-binding motifs, connected by a flexible linker.[2] Upon Ca^{2+}-binding, the conformation of CaM changes from the closed configuration to the open one, converting to a claviform dumbbell-shaped biomolecule with a long and rigid central helix connecting the N-lobe with the C-lobe, exposing much more hydrophobic and less negatively charged surfaces.[3] The exposed hydrophobic patches enable Ca^{2+}/CaM to recognize and bind with a wide range of target proteins.[4] Therefore, the conformation changes perform an essential part in Ca^{2+}-mediated signal transductions. Despite several techniques including NMR,[3a] X-ray crystallography,[3c] and single-molecule spectroscopy[5] were used to determine the conformations of CaM, technical complexity, expensive instruments, and veteran experimenter limit their extensive applications.

Graphene is a single-atom-thick nanosheet with 2D shape, which has been extensively explored with exciting applications.[6] Graphene oxide (GO)[7] decorated by oxygen-based functional groups has recently been widely used in biological applications,[8] resulting from the hybrid structure comprised of sp^2- and sp^3-hybridized carbon atoms that facilitate noncovalent interacting with biomolecules via electrostatic interactions, hydrophobic interactions or nonradiative dipole–dipole coupling.[9] Furthermore, GO exhibits amphiphilicity, excellent water dispersibility, efficient fluorescence quenching effect, and excellent surface functionalizability, enabling to perform as an optical probe for biosensing.[10] GO has been developed as an efficient platform for detection of biomolecules such as single-strand DNA,[11] microribonucleic acid (microRNA),[12] enzymes,[13] hormone,[14] denosine-5′-triphosphate (ATP),[15] and bioorganisms[16] by using GO with fluorescent dye-labeled nucleic acid, aptamers or peptide as probes. Due to the limited capability for recognition of these probes,[17] GO-based bioassays for sensing the conformation changes of proteins especially for CaM are still needed.

Water-soluble cationic-conjugated polymers (CCPs) are extensively employed in biological detections and fluorescence imaging by virtue of their light-harvesting properties and signal amplification properties.[18] Nilsson et al. have developed optical conformation probes to detect amyloid fibrils and calmodulin by using conjugated polythiophene and oligothiophene which is highly conformation sensitive.[19] Recently, we have used the optical properties of cationic polythiophene to visually detect the conformation change of CaM bound to synthetic peptide of M13.[20] However, this conjugated-polymer-based assay is only workable toward the hybrid protein of CaM-M13, and also exhibits high background signal arising from nonspecific

H. Yuan, Dr. J. Qi, Prof. C. Xing, Prof. H. An, R. Niu, Prof. Y. Zhan, Y. Fan, W. Yan, R. Li
Key Laboratory of Hebei Province for Molecular Biophysics
Institute of Biophysics
Hebei University of Technology
Tianjin 300401, P. R. China
E-mail: xingc@hebut.edu.cn; zhan_yong2014@163.com

H. Yuan, Prof. Y. Zhan
School of Materials Science and Engineering
Hebei University of Technology
Tianjin 300130, P. R. China

B. Wang, Prof. S. Wang
Key Laboratory of Organic Solids
Institute of Chemistry
Chinese Academy of Sciences
Beijing 100190, P. R. China
E-mail: wangshu@iccas.ac.cn

DOI: 10.1002/adfm.201501668

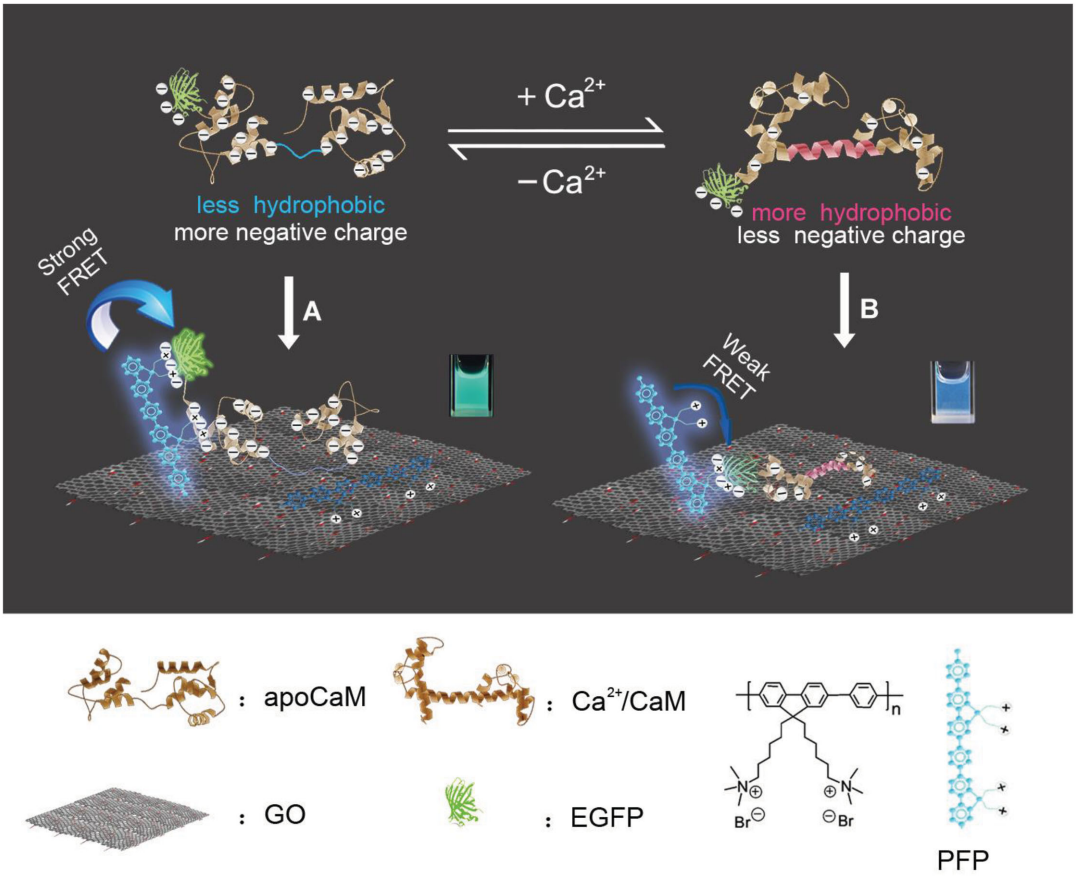

Scheme 1. Schematic representation of a GO-PFP-based hybrid probe for the detection of conformation changes of calmodulin.

interactions. CCPs have been found to have strong π–π interactions with GO and induce efficient fluorescence quenching effect.[21] Consequently, CCPs have recently been combined with GO for new biosensing systems with high signal-to-noise ratio.[17a,22] For example, Liu and co-workers demonstrated a graphene-conjugated oligomer hybrid probe for sensing of lectin and *Escherichia coli*.[17a] Here, we describe a hybrid probe of graphene oxide cationic conjugated polymer for detection of Ca^{2+}-induced conformation changes of calmodulin by using fluorescence resonance energy transfer (FRET) technique. As illustrated in **Scheme 1**, the CaM was labeled with enhanced green fluorescent protein (EGFP) at the N-terminus. Upon Ca^{2+}-binding, the conformation of CaM changes from the closed configuration to the open one, and the flexible linker converts to a rigid α-helix, resulting in the exposure of more hydrophobic and less negatively charge surface. Therefore, in contrast to the apoEGFP-CaM, the EGFP-CaM/Ca^{2+} can be assembled with GO tightly with stronger hydrophobic interaction and weaker electrostatic repulsion, leading to more EGFP-CaM/Ca^{2+} adsorption to the surface of GO. Upon adding PFP (poly[(9,9-bis(6′-*N*,*N*,*N*-trimethylammonium)hexyl)-fluorenylene phenylene dibromide]) to EGFP-CaM/Ca^{2+}/GO, the PFP resides in much farther proximity to EGFP than that in PFP/apoEGFP-CaM/GO, and therefore, much weaker FRET is observed in situation B than that in situation A. Interestingly, the assembly can be controlled by Ca^{2+} ions reversibly and circularly. Furthermore, the conformation changes of CaM and the Ca^{2+} controllable assembly of CaM with GO and PFP can be visualized directly in view of the color changes under UV irradiation.

2. Results and Discussion

2.1. Detection of the Conformation Changes of Calmodulin

PFP with a linear poly(fluorene)s backbone structure is used as the energy donor in FRET experiments, exhibiting an absorption maximum at 375 nm and an emission maximum at 420 nm, which overlaps with the absorption of EGFP.[23] Irradiation at 375 nm selectively excited PFP, and the FRET from PFP to EGFP leads to the fluorescence quenching of PFP at 420 nm and appearance of EGFP emission peak at 510 nm. As illustrated in **Figure 1**a, in the presence of GO, upon saturation of EGFP-CaM (1.0×10^{-6} M) with Ca^{2+} ions (5.0×10^{-3} M) and then PFP (7.5×10^{-6} M in repeat units (RUs)) was added, the resulting FRET ratio of the fluorescence intensity at 510 nm to that at 420 nm ($I_{510\ nm}/I_{420\ nm}$) shows a much lower signal than that for apoEGFP-CaM. However, in the absence of GO, both EGFP-CaM/Ca^{2+} and apoEGFP-CaM keep tight electrostatic

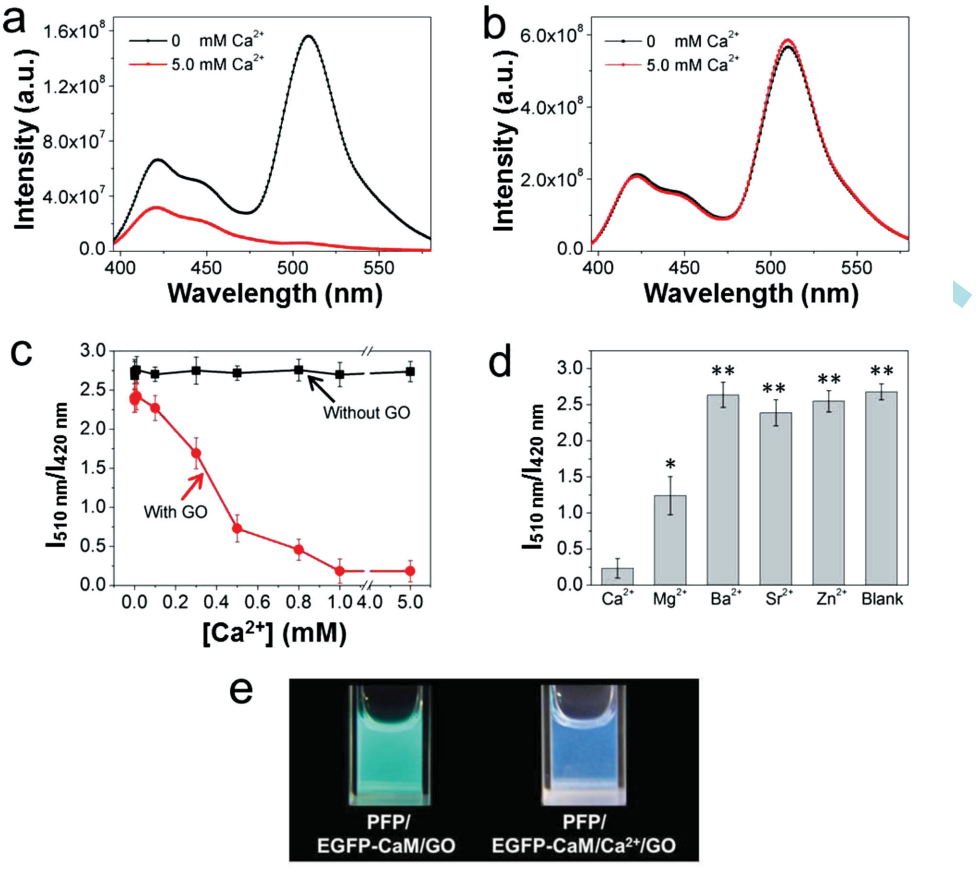

Figure 1. Fluorescence emission spectra of the PFP/EGFP-CaM in the a) presence and b) absence of GO with and without Ca^{2+}. c) Fluorescence emission ratio of $I_{510\ nm}/I_{420\ nm}$ of the PFP/EGFP-CaM in the presence and absence of GO as a function of Ca^{2+} concentrations. d) Fluorescence emission ratio of $I_{510\ nm}/I_{420\ nm}$ of PFP/EGFP-CaM in the presence of GO with various metal ions in HEPES buffer. e) Fluorescence images of the PFP/EGFP-CaM in the presence of GO with and without Ca^{2+} under UV light (λ_{max} = 365 nm). [GO] = 25.0 μg mL^{-1}, [EGFP-CaM] = 1.0×10^{-6} M, [PFP] = 7.5×10^{-6} M in repeat units (RUs), [metal ions] = 5.0×10^{-3} M, [Ca^{2+}] = 0–5.0×10^{-3} M. Measurements were performed in HEPES buffer solution (20.0×10^{-3} M, pH 7.4). The excitation wavelength is 375 nm. All data were presented as mean values ± standard deviation of three separate experiments. Error bars represent standard deviations of data from three separate measurements. Student's *t*-test was performed to determine statistical significance. Differences between groups were considered to be significant at *p*-values < 0.05, designated by *; and *p*-values < 0.01 by **.

interactions with PFP, and thus the observed FRET efficiency is not changed with adding Ca^{2+} ions (Figure 1b). Fluorescence emission ratio of $I_{510\ nm}/I_{420\ nm}$ of the PFP/EGFP-CaM in the presence and absence of GO as a function of Ca^{2+} concentrations was also examined. As exhibited in Figure 1c, in the presence of GO, the FRET ratio decreased gradually with the increase of the Ca^{2+} ions concentration and reached the plateau after about 1.0×10^{-3} M. However, the FRET ratio keep constant without GO. Figure 1d shows the fluorescence emission ratio ($I_{510\ nm}/I_{420\ nm}$) of PFP/EGFP-CaM in the presence of GO with various metal ions. For Ba^{2+}, Sr^{2+}, and Zn^{2+}, the FRET ratio values show slight changes relative to that of blank which was PFP/EGFP-CaM without metal ions, resulting from their weak binding abilities to CaM to produce conformation changes. For Mg^{2+} ions, the FRET ratio values was 50% decreased in contrast to the blank since Mg^{2+} ions can bind to CaM and induce a smaller conformational change than that of Ca^{2+} ions.[24] The FRET ratio for Ca^{2+} ions shows about 10 times lower relative to that for Ba^{2+}, Sr^{2+}, and Zn^{2+} ions and 5 times lower relative to that for Mg^{2+} ions. Therefore, this GO-PFP-based probe can be used to achieve detection of conformation changes of CaM specifically, and the detection limit can be lowered to 50.0×10^{-9} M by evaluating the FRET ratio changes of PFP/EGFP-CaM with Ca^{2+} relative to that without Ca^{2+} in the presence of GO as a function of EGFP-CaM concentration (Figure S1, Supporting Information). Notably, the fluorescence images of the PFP/EGFP-CaM in the presence of GO with and without Ca^{2+} under UV light show the color change from green to blue upon Ca^{2+}-binding (Figure 1e). In the control experiments, emission spectra of EGFP-CaM and PFP with and without GO as a function of Ca^{2+} concentrations were also measured (Figure S2, Supporting Information). The FRET results show the signal amplification by GO-PFP hybrid probe for detecting Ca^{2+}-induced conformation changes of calmodulin. The strategy of "premixing" or "postmixing" was studied to illustrate the each other interactions in our system. As shown in Figure S3 (Supporting Information), when EGFP-CaM and EGFP-CaM/Ca^{2+} were first mixed with PFP respectively and then GO was added,

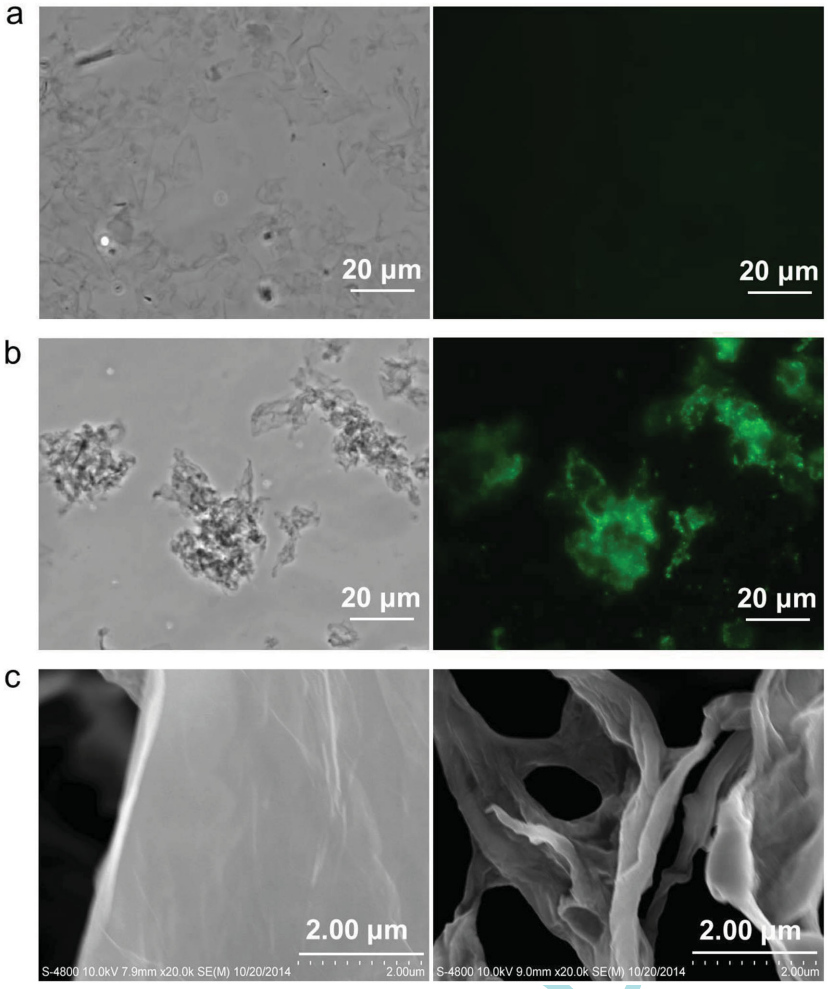

Figure 2. Phase contrast bright-field and fluorescence images of a) EGFP-CaM/GO and b) EGFP-CaM/Ca^{2+}/GO. Left: phase contrast bright-field images. Right: fluorescence images. Phase contrast images were taken at 20 ms exposure time and the fluorescence images were taken at 200 ms exposure time under EGFP filters. The false color of EGFP is green and the type of light filter is D470/40 nm exciter, 495 nm beamsplitter, and D525/50 nm emitter. The magnification of objective lens is 60×. c) SEM images of EGFP-CaM/GO (left) and EGFP-CaM/Ca^{2+}/GO (right) were observed at an accelerating voltage of 10.0 kV.

the FRET ratio values shows slight difference. Similarly, when PFP was first mixed with GO and then with EGFP-CaM and EGFP-CaM/Ca^{2+}, the fluorescence of PFP was quenched by GO greatly and the FRET ratio values illustrate no obvious changes as well. Therefore, in our protocol, EGFP-CaM and EGFP-CaM/Ca^{2+} must first assemble with GO respectively and then mix with PFP as illustrated in Scheme 1.

2.2. Mechanism Study of Calmodulin Sensing

To obtain further insight into the biosensing mechanism for CaM, the interactions of EGFP-CaM with GO were studied by phase contrast and fluorescence microscopy, as well as by scanning electron microscopy (SEM). As shown in **Figure 2**, EGFP-CaM/Ca^{2+} forms aggregates with GO, exhibiting bright fluorescence (Figure 2b); however, there was no obvious aggregation for apoEGFP-CaM in the presence of GO and little fluorescence can be observed (Figure 2a), which illustrates more EGFP-CaM/Ca^{2+} were absorbed on the surface of GO in comparison with apoEGFP-CaM. The SEM images indicate that the apoEGFP-CaM/GO complex has a regular and smooth surface (Figure 2c, left). Upon Ca^{2+}-binding, abundant absorption of EGFP-CaM/Ca^{2+} leads the surface of GO to become irregular, coarse, and wrinkled (Figure 2c, right). Because Ca^{2+}-binding induces the conformation of CaM to changes from the closed configuration to the open one, exposing more hydrophobic and less negatively charge surface, there is stronger binding of EGFP-CaM/Ca^{2+} with GO relative to that of apoEGFP-CaM. In addition, the SEM images of EGFP-CaM/Ca^{2+}/GO and EGFP-CaM/GO in the presence of PFP were also checked (Figure S4, Supporting Information), which indicates that the former triggers the formation of larger aggregates. Moreover, the assembly of EGFP-CaM with GO in the presence and absence of Ca^{2+} ions was also studied by atomic force microscopy (AFM). As shown in **Figure 3**, EGFP-CaM/GO forms well-dispersed nanosheets with a topographic height of ≈1.5 nm which is similar to that of single layered GO, and Ca^{2+}-binding induces large aggregates with undulating morphology and a topographic height of ≈50 nm. Furthermore, ζ potentials of EGFP-CaM with and without Ca^{2+} ions were examined in HEPES buffer. Table S1 (Supporting Information) demonstrates that the surface charges of EGFP-CaM became less when binding with Ca^{2+} ions. These results show that the EGFP-CaM/Ca^{2+} can be assembled with GO tightly with stronger hydrophobic interaction and weaker electrostatic repulsion, which induces different distance from PFP to EGFP-CaM/Ca^{2+} and apoEGFP-CaM, leading to different FRET efficiency for sensing CaM.

2.3. Reversibility Assay of Ca^{2+}-Controlled Assembly

To demonstrate the reversible assembly of EGFP-CaM with GO, ethylene glycol-bis(2-aminoethylether)-*N*,*N*,*N*′,*N*′-tetraacetic acid (EGTA) was used as a conductor to cycling Ca^{2+} ions concentration. **Figure 4**a shows that the FRET efficiency from PFP to EGFP was significantly quenched with Ca^{2+}-binding. However, after introduction of EGTA to chelate the Ca^{2+} ions subtotally, the FRET signal was recovered, indicating the disassembly of EGFP-CaM from GO. Moreover, the FRET ratio values of $I_{510\ nm}/I_{420\ nm}$ of the PFP/EGFP-CaM in the presence of GO versus different concentrations of Ca^{2+} upon cycling Ca^{2+}

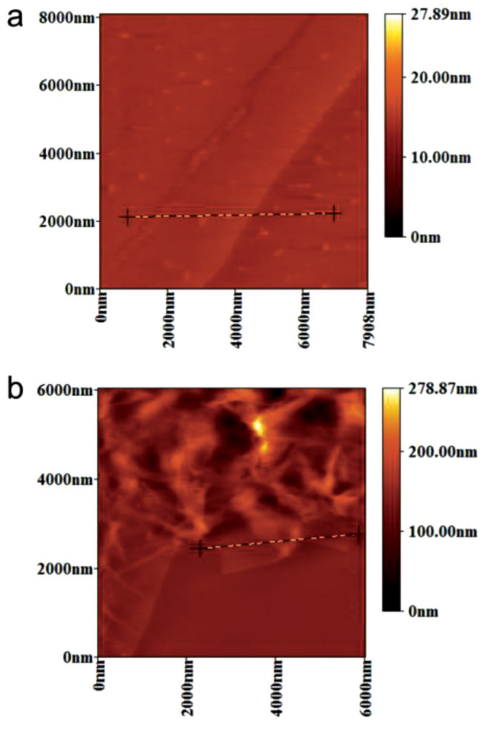

Figure 3. Atomic force microscopic images of a) EGFP-CaM/GO and b) EGFP-CaM/Ca^{2+}/GO. The line profile of the assembly shown in (a) and (b) are represented in the right, respectively.

were also examined. As shown in Figure 4b, it exhibits excellent circulatory change versus the concentrations of Ca^{2+} ions between 0 and 1.0×10^{-3} M, indicating that the assembly of EGFP-CaM with GO was controlled by Ca^{2+} ions quantitatively and reversibly.

2.4. Detection of CaM Binding to Target Peptide

In order to imitate the conformation change of CaM binding to target peptide in vivo, the 577 to 602 residues of skeletal myosin light-chain kinase called M13 was linked to the C-terminus of EGFP-CaM to obtain the hybrid protein of EGFP-CaM-M13.[25] Interestingly, fluorescence emission spectra of the PFP/EGFP-CaM-M13 in the presence of GO shows similar changes to that of EGFP-CaM upon binding with Ca^{2+} ions (**Figure 5**a). The curves of FRET ratio values of $I_{510\ nm}/I_{420\ nm}$ versus different concentrations of Ca^{2+} ions for EGFP-CaM-M13 were also similar to that of EGFP-CaM (Figure 5b). Therefore, GO-PFP hybrid probe can be applied to sensing the conformation changes of CaM binding to target peptide with FRET strategy. Moreover, the binding assay of EGFP-CaM-M13 with GO by phase contrast and fluorescence microscopy (Figure S5, Supporting Information) and the reversible assembly of EGFP-CaM-M13 with GO controlled by Ca^{2+} ions (Figure S6, Supporting Information) were detected as well.

3. Conclusion

In summary, we have demonstrated a graphene oxide-cationic conjugated polymer hybrid probe for sensing the conformation transition of CaM with high signal-to-noise ratio. This new, simple, visualized, and cost-effective assay has several significant features. First, the assembly of EGFP-CaM with GO is dominated by the electrostatic and hydrophobic interactions, without any covalent linkage of chemical ligands, which reduces complicated synthesis procedures. Second, the assembly of EGFP-CaM with GO is quantitatively and reversibly controlled by Ca^{2+} ions. Third, the GO-PFP hybrid probe can be workable not only for calmodulin but also for calmodulin binding to target peptide which imitates the transformation in vivo. Furthermore, the transition of calmodulin is directly visualized with naked eye by the fluorescence color changes under UV light. Thus, GO-PFP-based assay for calmodulin by applying FRET technique

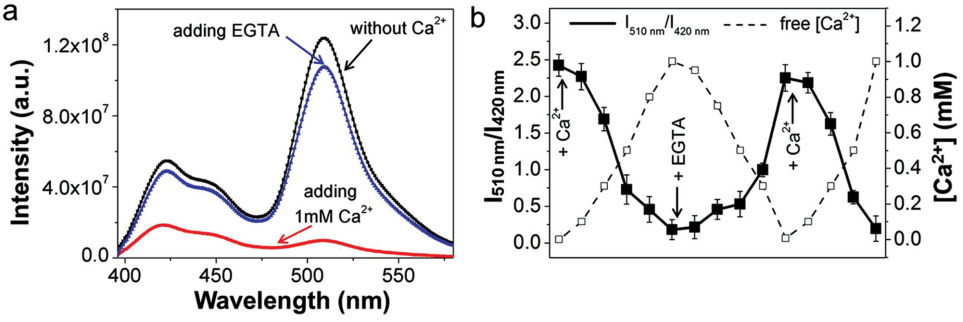

Figure 4. a) Fluorescence emission spectra of the PFP/EGFP-CaM in the presence of GO upon adding Ca^{2+} and EGTA in HEPES buffer solution. b) Fluorescence emission ratio of $I_{510\ nm}/I_{420\ nm}$ of the PFP/EGFP-CaM in the presence of GO versus different concentrations of Ca^{2+} upon cycling Ca^{2+}. Solid line represents the FRET ratio values of $I_{510\ nm}/I_{420\ nm}$ and dashed line represents the concentration of Ca^{2+}. [GO] = 25.0 μg mL^{-1}, [EGFP-CaM] = 1.0×10^{-6} M, [PFP] = 7.5×10^{-6} M in repeat units (RUs), [Ca^{2+}] = 0–1.0×10^{-3} M. Measurements were performed in HEPES buffer solution (20.0×10^{-3} M, pH 7.4). The excitation wavelength is 375 nm.

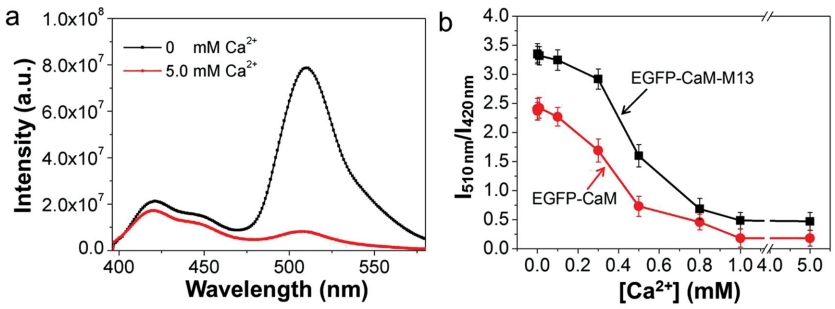

Figure 5. a) Fluorescence emission spectra of the PFP/EGFP-CaM-M13 in the presence of GO with and without Ca^{2+}. b) Fluorescence emission ratio of $I_{510\ nm}/I_{420\ nm}$ of the PFP/EGFP-CaM and PFP/EGFP-CaM-M13 in the presence of GO as a function of Ca^{2+} concentrations. [GO] = 25.0 μg mL^{-1}, [EGFP-CaM] = [EGFP-CaM-M13] = 1.0×10^{-6} M, [PFP] = 7.5×10^{-6} M in repeat units (RUs), [Ca^{2+}] = 0–5.0×10^{-3}M. Measurements were performed in HEPES buffer solution (20.0×10^{-3} M, pH 7.4). The excitation wavelength is 375 nm.

exhibits high potential as diagnostic materials for sensing conformation changes in biomolecular process.

4. Experimental Section

Materials and Reagents: PFP was prepared according to a literature procedure.[26] Graphene oxide was prepared from natural graphitic powder according to Hummer's method and exfoliated into GO by sonication in water.[27] Graphite powder, sulfuric acid, hydrogen peroxide, potassium permanganate, potassium persulfate, and phosphorus pentoxide were purchased from Tianjin Guangfu Ltd. Standard $CaCl_2$ (1.0 M), EGTA, HEPES (4-(2-Hydroxyethyl)piperazine-1-ethanesulfonic acid), and 96 well were purchased from Sigma. The others were obtained from Aladdin, Acros, or Alfa-Aesar and used as received. All solutions were prepared with Milli-Q water.

Characterizations of GO: As shown in Figure S7 (Supporting Information), the GO sheets were mostly single layered (topographic height ≈1.4 nm, similar to earlier studies) and about 6000 nm in lateral width according to atomic force microscopy (AFM) characterization. The XPS spectra of the GO confirmed the presence of C, O, and the carbon-to-oxygen (C/O) atomic ratio is 2.8.

Instruments: Fluorescence measurements were measured on a SpectraMax i3 Multi-mode microplate detection platform (Molecular Devices, USA) with a Xenon lamp excitation source. Phase contrast bright-field and fluorescence images were taken on a fluorescence microscope (Nikon TiU) with a mercury lamp (100 W) as light source. The excitation wavelength was 470/40 nm for EGFP. Photographs were taken with a Canon EOS-600D digital camera. The morphologies of the EGFP-CaM on GO were observed on a JEOL JSM 4800F field-emission scanning electron microscope. AFM images were taken by CSPM 5000 scanning probe microscope in tapping mode. XPS data were taken by Perkin-Elmer PHI 1600 spectrometer. ζ potentials experiments were carried out on Nano-ZS90 (Malvern Instruments, UK).

EGFP-CaM and EGFP-CaM-M13 Preparation: The cDNA of the EGFP was amplified by the polymerase chain reaction (PCR) with a sense primer containing Nde I site and a reverse primer containing Xho I site. M13 was synthesized by Takara Ltd. The fusion DNA fragments of EGFP-CaM and EGFP-CaM-M13 were cloned into the pCold II plasmid, expressed in *E. coli* (BL21 strain), purified, dialyzed, and quantified finally according to a reported method.[28]

Preparation of HEPES Buffer: For zero-Ca^{2+} buffer, the solution contained 20.0×10^{-3} M HEPES and 20.0×10^{-6} M EGTA was adjusted to pH 7.4 with NaOH. For high-Ca^{2+} buffer, the solution contained 20.0×10^{-3} M HEPES, 20.0×10^{-6} M EGTA and 100.0×10^{-3} M $CaCl_2$ was adjusted to pH 7.4 with NaOH. Different concentrations of free Ca^{2+} solutions were made by mixing zero-Ca^{2+} and high-Ca^{2+} solutions according to the Ca-EGTA calculator (http://www.stanford.edu/~cpatton/CaEGTA-NIST.htm).

Detection of the Conformation Changes of Calmodulin: 5.0 μL of 40.0×10^{-6} M EGFP-CaM stock solution was added in 200 μL of HEPES buffer with different concentrations of free Ca^{2+} (0–5.0×10^{-3} M) respectively and incubated for 10 min, and then 10.0 μL of 0.5 mg mL^{-1} GO was added into the well and mixed gently. After the mixtures were incubated for 30 min at room temperature, PFP (7.5×10^{-6} M in repeat units (RUs)) was added and incubated for 10 min. These samples were measured the fluorescence spectra in 96-well microplate through a multimode detection platform. The excitation wavelength is 375 nm.

Morphology Study of EGFP-CaM with GO: 25.0 μL of 40.0×10^{-6} M EGFP-CaM stock solution was added in 1.0 mL of HEPES buffer with 0 and 5.0×10^{-3} M Ca^{2+} respectively and incubated for 10 min, then 25.0 μg mL^{-1} GO was added into the well and mixed gently. After the mixtures were incubated for 30 min at room temperature, the samples were centrifuged for 15 min at 8000 r, 4 °C, and the supernate was removed. Then, the precipitates were resuspended in 20 μL sterile water. Phase contrast bright-field and fluorescence images were taken on a fluorescence microscope. The phase contrast images were taken at 20 ms and the fluorescence images were taken at 200 ms under EGFP filters. The false color of EGFP is green and the type of light filter is D470/40 nm exciter, 495 nm beamsplitter, and D525/50 nm emitter. The magnification of objective lens is 60×. SEM images were observed on a JEOL JSM 4800F field-emission scanning electron microscope, at an accelerating voltage of 10.0 kV.

Reversibility Assay of Assembly of EGFP-CaM with GO: Ca^{2+} ions ([Ca^{2+}] = 0–1.0×10^{-3} M) was added successively to a solution with EGFP-CaM (1.0×10^{-6} M) and GO (25.0 μg mL^{-1}) in zero-Ca^{2+} buffer. When the concentration of Ca^{2+} increases to 1.0×10^{-3} M, different volume of 10.0×10^{-3} M EGTA were dropped into the wells to decrease the concentration of Ca^{2+}, then Ca^{2+} ions was recovered through added high-Ca^{2+} buffer. For cycling Ca^{2+} ions, the accurate concentration of Ca^{2+} was calculated according to the Ca-EGTA calculator, and the measurement of fluorescence spectra was same to the previous procedure.

Supporting Information

Supporting Information is available from the Wiley Online Library or from the author.

Acknowledgements

The authors are grateful for the financial support of the Scientific Innovation Grant for Excellent Young Scientists of Hebei University of Technology (Grant No. 2013003), "100 Talents" Program of Hebei Province, China (Grant No. E2014100004), Program for Excellent Innovative Talents in Universities of Hebei Province, China (Grant No. BJ2014011), Hebei Province Science Foundation (Grant Nos. QN2014024 and No. B2015202330), and the National Natural Science Foundation of China (Grant No. 21373243).

Received: April 25, 2015
Published online: June 5, 2015

[1] a) D. Chin, A. R. Means, *Trends Cell Biol.* **2000**, *10*, 322; b) D. E. Clapham, *Cell* **2007**, *131*, 1047.
[2] a) Y. Ogawa, M. Tanokura, *J. Biochem.* **1984**, *95*, 19; b) W. E. Meador, A. R. Means, F. A. Quiocho, *Science* **1993**, *262*, 1718; c) H. Kuboniwa, N. Tjandra, S. Grzesiek, H. Ren, C. B. Klee, A. Bax, *Nat. Struct. Biol.* **1995**, *2*, 768.
[3] a) M. Ikura, G. M. Clore, A. M. Gronenborn, G. Zhu, C. B. Klee, A. Bax, *Science* **1992**, *256*, 632; b) M. Zhang, T. Tanaka, M. Ikura, *Nat. Struct. Biol.* **1995**, *2*, 758; c) Y. S. Babu, C. E. Bugg, W. J. Cook, *J. Mol. Biol.* **1988**, *204*, 191; d) H. Sun, D. Yin, T. C. Squier, *Biochemistry* **1999**, *38*, 12266.
[4] a) B. E. Finn, S. Forsen, *Structure* **1995**, *3*, 7; b) S. W. Vetter, E. Leclerc, *Eur. J. Biochem.* **2003**, *270*, 404.
[5] B. D. Slaughter, J. R. Unruh, M. W. Allen, R. J. Bieber Urbauer, C. K. Johnson, *Biochemistry* **2005**, *44*, 3694.
[6] a) K. S. Novoselov, A. K. Geim, S. V. Morozov, D. Jiang, Y. Zhang, S. V. Dubonos, I. V. Grigorieva, A. A. Firsov, *Science* **2004**, *306*, 666; b) X. Huang, X. Qi, F. Boey, H. Zhang, *Chem. Soc. Rev.* **2012**, *41*, 666; c) M. Pumera, *Mater. Today* **2011**, *14*, 308; d) K. Yang, L. Feng, X. Shi, Z. Liu, *Chem. Soc. Rev.* **2013**, *42*, 530; e) K. Kostarelos, K. S. Novoselov, *Science* **2014**, *344*, 261.
[7] K. S. Kim, Y. Zhao, H. Jang, S. Y. Lee, J. M. Kim, J. H. Ahn, P. Kim, J. Y. Choi, B. H. Hong, *Nature* **2009**, *457*, 706.
[8] a) K. P. Loh, Q. Bao, G. Eda, M. Chhowalla, *Nat. Chem.* **2010**, *2*, 1015; b) Y. Wang, Z. Li, J. Wang, J. Li, Y. Lin, *Trends Biotechnol.* **2011**, *29*, 205.
[9] a) D. R. Dreyer, S. Park, C. W. Bielawski, R. S. Ruoff, *Chem. Soc. Rev.* **2010**, *39*, 228; b) J. Kim, L. J. Cote, F. Kim, J. Huang, *J. Am. Chem. Soc.* **2010**, *132*, 260.
[10] a) C. Chung, Y.-K. Kim, D. Shin, S.-R. Ryoo, B. H. Hong, D.-H. Min, *Acc. Chem. Res.* **2013**, *46*, 2211; b) X. Deng, H. Tang, J. Jiang, *Anal. Bioanal. Chem.* **2014**, *406*, 6903; c) H. Dong, W. Gao, F. Yan, H. Ji, H. Ju, *Anal. Chem.* **2010**, *82*, 5511; d) J. Qi, W. Lv, G. Zhang, Y. Li, G. Zhang, F. Zhang, X. Fan, *Nanoscale* **2013**, *5*, 6275.
[11] a) Q. Wang, N. Xu, J. Lei, H. Ju, *Chem. Commun.* **2014**, *50*, 6714; b) E. Morales-Narvaez, A. Merkoci, *Adv. Mater.* **2012**, *24*, 3298; c) X. Liu, F. Wang, R. Aizen, O. Yehezkeli, I. Willner, *J. Am. Chem. Soc.* **2013**, *135*, 11832; d) C.-H. Lu, H.-H. Yang, C.-L. Zhu, X. Chen, G.-N. Chen, *Angew. Chem. Int. Ed.* **2009**, *48*, 4785; e) X. Li, K. Ma, S. Zhu, S. Yao, Z. Liu, B. Xu, B. Yang, W. Tian, *Anal. Chem.* **2013**, *86*, 298.
[12] a) Z. Lu, L. Zhang, Y. Deng, S. Li, N. He, *Nanoscale* **2012**, *4*, 5840; b) S.-R. Ryoo, J. Lee, J. Yeo, H.-K. Na, Y.-K. Kim, H. Jang, J. H. Lee, S. W. Han, Y. Lee, V. N. Kim, D.-H. Min, *ACS Nano* **2013**, *7*, 5882.
[13] a) H. Chang, L. Tang, Y. Wang, J. Jiang, J. Li, *Anal. Chem.* **2010**, *82*, 2341; b) H. Jang, Y.-K. Kim, H.-M. Kwon, W.-S. Yeo, D.-E. Kim, D.-H. Min, *Angew. Chem. Int. Ed.* **2010**, *49*, 5703.
[14] Y. Pu, Z. Zhu, D. Han, H. Liu, J. Liu, J. Liao, K. Zhang, W. Tan, *Analyst* **2011**, *136*, 4138.
[15] Y. He, Z.-G. Wang, H.-W. Tang, D.-W. Pang, *Biosens. Bioelectron.* **2011**, *29*, 76.
[16] a) S. Liu, T. H. Zeng, M. Hofmann, E. Burcombe, J. Wei, R. Jiang, J. Kong, Y. Chen, *ACS Nano* **2011**, *5*, 6971; b) J. Li, L.-J. Wu, S.-S. Guo, H.-E. Fu, G.-N. Chen, H.-H. Yang, *Nanoscale* **2013**, *5*, 619.
[17] a) L. Wang, K.-Y. Pu, J. Li, X. Qi, H. Li, H. Zhang, C. Fan, B. Liu, *Adv. Mater.* **2011**, *23*, 4386; b) Q. Xu, H. Cheng, J. Lehr, J. J. Davis, *Anal. Chem.* **2015**, *87*, 346.
[18] a) F. Wang, Z. Liu, B. Wang, L. Feng, L. Liu, F. Lv, Y. Wang, S. Wang, *Angew. Chem. Int. Ed.* **2014**, *53*, 424; b) L. H. Feng, C. L. Zhu, H. X. Yuan, L. B. Liu, F. T. Lv, S. Wang, *Chem. Soc. Rev.* **2013**, *42*, 6620; c) C. Xing, H. Yuan, S. Xu, H. An, R. Niu, Y. Zhan, *ACS Appl. Mater. Interfaces* **2014**, *6*, 9601; d) S. Rochat, T. M. Swager, *J. Am. Chem. Soc.* **2013**, *135*, 17703.
[19] a) A. Herland, K. P. R. Nilsson, J. D. M. Olsson, P. Hammarström, P. Konradsson, O. Inganäs, *J. Am. Chem. Soc.* **2005**, *127*, 2317; b) K. P. R. Nilsson, O. Inganas, *Macromolecules* **2004**, *37*, 9109; c) S. Nyström, K. M. Psonka-Antonczyk, P. G. Ellingsen, L. B. G. Johansson, N. Reitan, S. Handrick, S. Prokop, F. L. Heppner, B. M. Wegenast-Braun, M. Jucker, M. Lindgren, B. T. Stokke, P. Hammarström, K. P. R. Nilsson, *ACS Chem. Biol.* **2013**, *8*, 1128.
[20] H. Yuan, C. Xing, H. An, R. Niu, R. Li, W. Yan, Y. Zhan, *ACS Appl. Mater. Interfaces* **2014**, *6*, 14790.
[21] X. J. Xing, Y. Zhou, X. G. Liu, H. W. Tang, D. W. Pang, *Analyst* **2013**, *138*, 6301.
[22] a) X. J. Xing, X. G. Liu, Y. He, Y. Lin, C. L. Zhang, H. W. Tang, D. W. Pang, *Biomacromolecules* **2012**, *14*, 117; b) J. Geng, L. Zhou, B. Liu, *Chem.Commun.* **2013**, *49*, 4818.
[23] a) C. Wang, Y. Tang, Y. Liu, Y. Guo, *Anal. Chem.* **2014**, *86*, 6433; b) B. Liu, S. Wang, G. C. Bazan, A. Mikhailovsky, *J. Am. Chem. Soc.* **2003**, *125*, 13306; c) C. Xing, L. Liu, Z. Shi, Y. Li, S. Wang, *Adv. Funct. Mater.* **2010**, *20*, 2175; d) F. Pu, D. Hu, J. Ren, S. Wang, X. Qu, *Langmuir* **2010**, *26*, 4540; e) X. Duan, L. Liu, X. Feng, S. Wang, *Adv. Mater.* **2010**, *22*, 1602.
[24] K. B. Seamon, *Biochemistry* **1980**, *19*, 207.
[25] a) A. Miyawaki, J. Llopis, R. Heim, J. M. McCaffery, J. A. Adams, M. Ikura, R. Y. Tsien, *Nature* **1997**, *388*, 882; b) K. Truong, A. Sawano, H. Mizuno, H. Hama, K. I. Tong, T. K. Mal, A. Miyawaki, M. Ikura, *Nat. Struct. Biol.* **2001**, *8*, 1069.
[26] a) B. Liu, S. Wang, G. C. Bazan, A. Mikhailovsky, *J. Am. Chem. Soc.* **2003**, *125*, 13306; b) C. Xing, L. Liu, Z. Shi, Y. Li, S. Wang, *Adv. Funct. Mater.* **2010**, *20*, 2175; c) F. Pu, D. Hu, J. Ren, S. Wang, X. Qu, *Langmuir* **2010**, *26*, 4540; d) X. Duan, L. Liu, X. Feng, S. Wang, *Adv. Mater.* **2010**, *22*, 1602.
[27] a) S. Park, R. S. Ruoff, *Nat Nano* **2009**, *4*, 217; b) J. Qi, W. Lv, G. Zhang, F. Zhang, X. Fan, *Polym. Chem.* **2012**, *3*, 621.
[28] K. M. Arndt, K. M. Müller, *Protein Engineering Protocols*, Humana Press, Totowa, NJ **2007**.